DEVELOPMENT OF HYBRID FOG DETECTION ALGORITHM USING VARIOUS FOG CHARACTERISTICS

Ji-Hye Han (1), Myoung-Seok Suh (1), Na-Young Roh (1), Ha-Yeong Yu (1)

[1] Kongju National Univ., 32588 56, Gongjudaehak-ro, Gongju-si, Chungcheongnam-do, Korea
Email: gihh1131@smail.kongju.ac.kr; sms416@kongju.ac.kr;
rohna0368@smail.kongju.ac.kr; hakkk96@smail.kongju.ac.kr

KEY WORDS: Fog, GK2A/AMI, Himawari-8/AHI, visibility

ABSTRACT: To develop the fog detection algorithm using the GK2A/AMI, we developed a hybrid fog detection algorithm (HFDA) using various fog characteristics with Himawari-8/AHI as proxy data. Since the available satellite channels vary with time, and the fog has various characteristics depending on the geographical location, we developed an HFDA according to the time and geographical location. The difference between reflectance and composited reflectance for 30 days and the difference in emissivity between SWIR and IR channels were mainly used. To overcome the difficulty of distinguishing low clouds from fog, we used the difference between the fog top temperature(BT11) and simulated brightness temperature of clear sky(CSR_BT11) as the ground temperature data. The fog was detected by using a decision tree method based on the combinations of multi-channels. The visual comparison showed that the fog detection results of this study detect local fog better than that of COMS. In quantitative validation using visibility meter data for 16 training cases and 6 validation cases, the average PODs are 0.77 and 0.74, respectively. However, FAR is also very high(0.77 and 0.89). Especially, the POD and FAR in summer are low and high regardless of training and validation cases. Geographically, PODs of coast area are lower than that over land. The lower performance of HFDA at the coastal area is mainly caused by the complexity of background properties of the coastal area due to the mixture of land and sea.

1. INTRODUCTION

Fog is a meteorological phenomenon caused by the condensation of water droplets or super-cooled water droplets or ice crystals like a cloud. Unlike clouds, as the fog occurs near the Earth's surface, that affects various form of human activities such as traffic systems and production to crops and cultural assets. Therefore, to reduce the damage caused by fog, improvement of detection and forecasting in real time (or near real time) is very important. The characteristics of fog vary with time, surface type, season, and mechanism of occurrence. Besides, the fog varies in intensity and duration depending on particle size and water concentration, etc. Fog studies were performed primarily based on surface type. In the fog cases on land that occur locally, most of researches using ground observation data were performed(Lee and Ahn, 2013). On the other hand, in the sea fog cases, the researches using satellite data were mainly performed because the ground observation data were not available(Shin et al., 2013). In this way, the fog was studied mainly by classifying land fog or sea fog according to surface type, or to analyze fog characteristics according to particle size or water concentration using a model(Gultepe et al., 2006).

As the characteristics of fog are various, the fog detection methods using various data have been proposed. However, the ground observation data has a problem of spatial representation, and the numerical model has a problem of accuracy and the inability to detect the fog in real time. So, a lot of researches carried out using geostationary satellite for analysis or detection of the fog because it is possible to detect or short-term forecast for a large area (Lee et al., 2011). Early researches for fog detection from satellite data used the reflectance in daytime and brightness temperature in nighttime (Ellord 1995; Ahn et al., 2003). Since only a single channel had the limitation of fog detection at night, Eyre et al. (1995) proposed a method using the difference between two infrared channels to distinguish between fog and other clouds at night (Ellrod, 1995). The emissivity of shortwave infrared channels (3.7 ~ 3.9 um) has around 0.8 ~ 0.9 for water droplets while that of infrared window channels have close to 1.0 (Shin et al., 2012). Therefore, the temperature difference between the two channels (DCD; Dual Channel Difference) can be used to distinguish fog from other objects (Kim et al., 2018). Because the DCD is very effective in fog detection at nighttime, it is still used in many fog studies (Park and Kim, 2012; Shin et al., 2013).

However, fog detection using the only reflectance and DCD at day/night, there is a limit to distinguish fog and others such as low clouds, partly clouds, cirrus, snow, etc (Kim et al., 2018; Han et al., 2019). To overcome this problem, various methods using various characteristics of fog have been attempted (Shin et al., 2013). The optical and textual characteristics of fog are well documented in Suh et al. (2017). Fog usually occurs when the atmosphere is stable, so the top of fog is homogeneous and the altitude is low. Therefore local standard deviation(LSD) and difference of fog top temperature and ground temperature(ΔFTs) are often used to distinguish them from other clouds(Park and Kim, 2012; Shin et al., 2013; Kim et al., 2018; Han et al., 2019). To reduce false detected high clouds, in particular, cirrus,

the difference of two infrared window channels (10.8 um − 12.0 um) is utilized(Lee et al., 2011). In addition, it is possible to improve the detection level of fog by using various fog characteristics using geostationary satellite such as normalized difference snow index(NDSI), 8.6 um, CO2 channel utilization (Choi, 2007; Jeon et al., 2016).

Recently, GEO-KOMPSAT-2A(GK2A), Korea's second geostationary meteorological satellite was launched in December, 2018. The satellite has higher spatio-temporal resolution and better spectral resolution than the existing the Communication, Ocean, and Meteorological Satellite(COMS). The advanced meteorological imager(AMI) loaded on GK2A observes the full disk area every 10 minutes and is equipped with 4 visible channels from 500 m to 1 km spatial resolution and 12 infrared or near-infrared channels with 2 km resolution(NMCS, 2019). In particular, as the number of channels is greatly improved compared to that of COMS, fog detection using various characteristics of the fog is possible.

Therefore, in this study, we developed a fog detection algorithm(HFDA) using various fog characteristics that can be analyzed from the GK2A/AMI data. Decision tree method used in this study for fog detection requires various fog cases. However, because the data of GK2A is not enough, we developed a fog detection algorithm using Himawari-8/Advanced Himawari Imager(AHI) of Japan's geostationary satellite launched in 2015 as a proxy data. To consider the variable characteristics of fog, HFDA was developed according to time(day, dawn/twilight, and night) and surface type(land, sea, and coast). In section 2, the data and method used in this study are explained. And the results of fog detection using satellite data and the conclusion of this study are shown in section 3 and section 4, respectively.

2. DATA AND METHOD

2.1 Data

For fog detection, the Himawari-8/AHI data provided by the National Meteorological Satellite Center(NMSC) of the Korea Meteorological Administrator(KMA) were used. The Himawari-8 observes a full disk every 10 minutes and has 16 channels including 4 visible channels, 2 near infrared channels, 1 shortwave infrared channel, 3 water vapor channels, and 6 infrared channels(Bessho et al., 2016). Table 1 shows the information of the Himawari-8/AHI's and GK2A/AMI's channels used in this study

To reduce false detected low clouds, brightness temperature of clear sky radiance(CSR_BT11) provided by NMSC was used as ground temperature. The CSR_BT11 is simulated by the radiative transfer model using temperature and humidity profile of UM model as input data (Han, 2018). This data has a spatial resolution of 17 km and a temporal resolution of 1 hour, and was used after interpolating 2 km to fit the satellite pixels (Kim et al., 2018).

Variability of the fog is highly depending on the mechanisms and area of occurrence (Lee, 2016). Therefore, in this study, we developed algorithms according to the area of occurrence using land sea mask. The land sea mask provided by NMSC, which was divided only by land and sea, was reclassified into land, sea, and coast for the fog detection(Fig. 1).

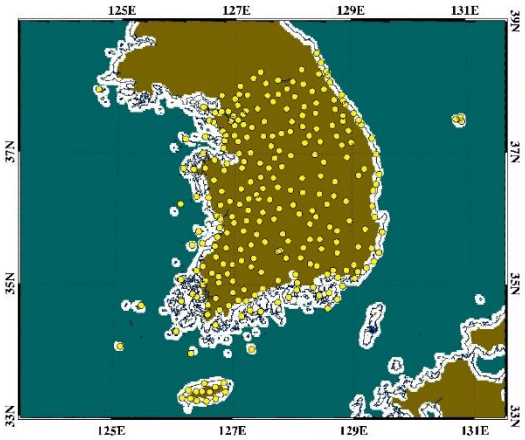

Figure 1. Spatial distribution of visibility meter data(yellow dot) with land sea mask. White shaded pixels are coast area, blue color pixels are sea, and brown color pixels are land.

Visibility meter data provided by the KMA were used to quantitatively validate the fog detection algorithm developed in this study. As shown in Fig. 1, the visibility meter installed at about 280 stations in South Korea observe the horizontal visibility every 1 minutes (Lee and Suh, 2018). Since spatio-temporal resolution of satellite data and visibility data are different, colocation process is necessary (Kim et al., 2018). Therefore, 10 min averaged visibility data was used and verified with the nearest satellite pixel based on the visibility data.

To develop the fog detection algorithm and set threshold values, A total of 22 fog cases are chosen according to season and intensity to consider the diversity of the fog. Of these, 16 were selected as training cases and the others were selected

as validation cases.

Table 1. Channel characteristics of AMI/GK2A and AHI/Himawari-8

Channel	Center wavelength (μm)		Spatial resolution (km)	Temporal frequency (minutes)
	AMI	AHI		
VIS	0.64	0.64	0.5	10
NIR	1.6	1.6	2	10
SWIR	3.8	3.9	2	10
IR	8.7	8.6	2	10
IR	10.5	10.4	2	10
IR	11.2	11.2	2	10
IR	12.3	12.3	2	10
IR	13.3	13.3	2	10

2.2 Method

Figure 2 shows a flow chart of the fog detection algorithm developed in this study. As shown in Fig.2, it has consisted of online and offline processes. In offline process, the initial and optimized threshold values are determined. And the fog detection using optimized threshold values and validation are performed in real-time.

Since availability of satellite data is different between daytime and nighttime, time discontinuity is inevitable after sunrise/sunset (Schreiner et al., 2007). Therefore, in this study, the fog detection is performed separately according to the solar zenith angle (SZA: day, night, and dawn/twilight) (Suh et al., 2017). To minimize the time discontinuity between day and night, the previous results of the fog detection were used during the dawn/twilight(when the SZA is between 70° and 95°) (Park, 2012). In addition, fog or reference properties are highly influenced by the surface type, the fog detection is performed separately according to the surface type(land, sea, and coast) as well as time. To solve the spatial discontinuity, both the sea fog detection algorithm and the land fog detection algorithm are applied for the coastal area.

Nine test elements were used to detect the fog using decision tree method. Among them, difference between reflectance of 0.64 um and composited reflectance of 0.64 um for 30 days(ΔVIS) and DCD was used in daytime and nighttime, respectively. Reflectance data, which is used primarily during the day, **has limitation** in distinguishing fog from clear pixels when an SZA is high. Therefore, in this study, the reflectance data composited for 30 days by minimum value composite method was utilized. Although satellite's capability is greatly improved, satellite alone has limitations in detecting fog with various characteristics, numerical model data(CSR_BT11) are used to detect fog. To distinguish between low cloud and fog, ΔFTs using CSR_BT11 was used regardless of time and surface type. Also, in order to remove other clouds, local standard deviation (LSD), difference between BT10.4 with BT12.3(BTD2) using water vapor absorption difference between two window channels, and the rate of change for DCD were used. In addition, normalized difference snow index(NDSI), difference between BT8.6 and BT11.2(BTD3) with characteristics similar to DCD, difference between BT13.3 and BT11.2(BTD1) with CO2 absorption channel were used to remove the remaining false detected clear pixels.

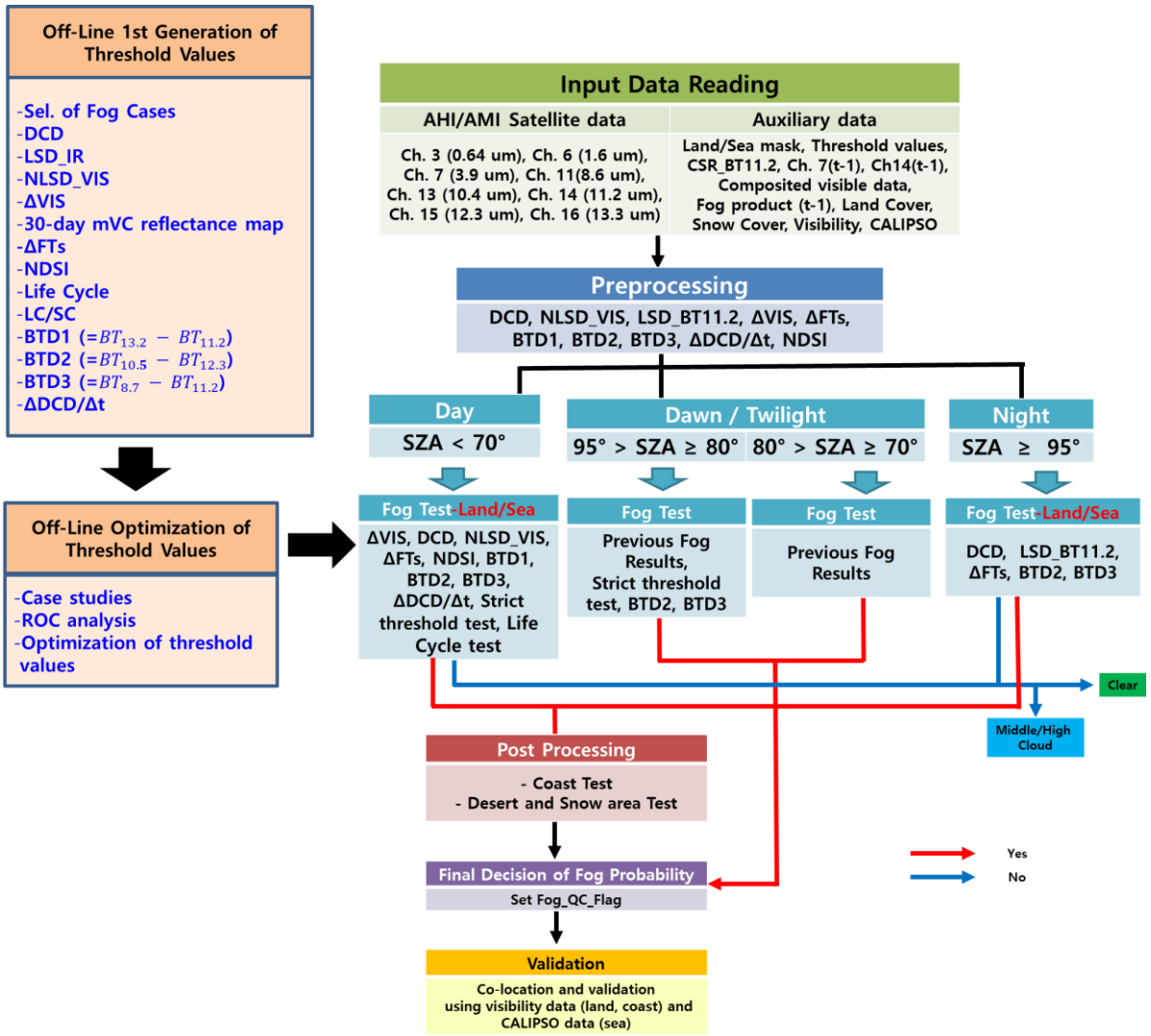

Figure 2. Flow chart of fog detection algorithm using AHI of Himawari-8.

To determinate initial threshold values of test elements, we analyzed frequency distribution of each test element according to time and surface type. Figure 3 shows sample image of frequency distribution for ΔVIS and DCD. The ΔVIS value ranges from 0 to 20 % and 10 to 20 % in the land and the coast, respectively. Most of the DCD values in nighttime are less than 0 K irrespective of the geographic location. At the dawn, the DCD values show higher values than night due to the influx of solar radiation. The initial threshold value set by frequency analysis was optimized through ROC analysis. The optimized thresholds are shown in Table 2 and used as initial thresholds for GK2A/AMI.

And, the visibility data, that ground observation data, was used to determine the threshold values and quantitatively validation for the detection level of HFDA.

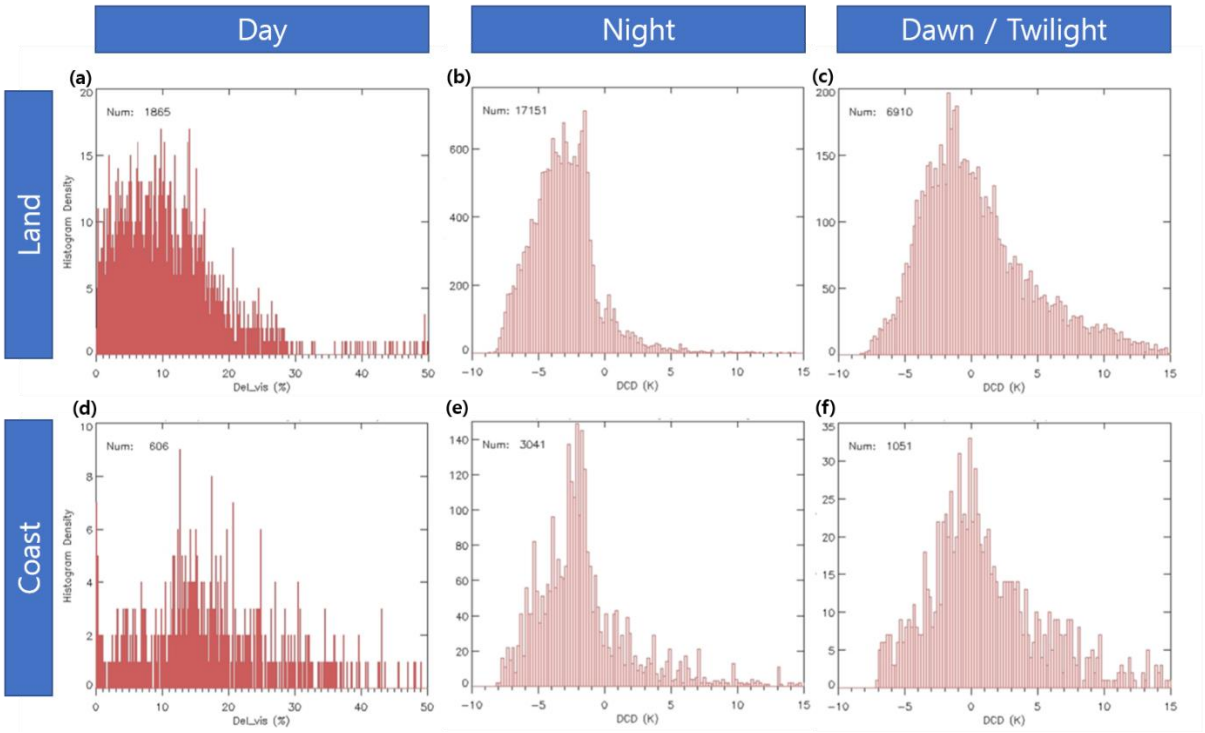

Figure 3. Frequency distribution of ΔVIS and DCD according to time and geographic location. (a) ~ (c) and (d) ~ (f) graphs represent the frequency on land and coast, respectively. And (a) and (d) graphs show a frequency in daytime, (b) and (e) show in nighttime, and (c) and (f) show in dawn/twilight.

Table 2. Initial and optimized threshold values of test elements.

	Night		**Day**			**Dawn**		
	Land	Sea	Land		Sea	Land		Sea
DCD [K]	-1.5	-0.5	-1.0~15.0					
ΔVIS [%]			2.0 & 35.0		2.0 & 40.0			
ΔFTs [K]	5.0	6.0	-1.0~-4.0 & 5.0		6.0			
LSD [K]	2.0	1.0						
NLSD			0.8		0.3			
BTD3 [K]	-1.3	-1.3	-1.3		-1.3	-1.3		
BTD2 [K]	3.0	3.0	3.0		4.0	3.0		3.0
BTD1 [K]	-19.0		-19.0					
DCD ratio [K/10min]			-0.14 & 0.35					
NDSI			-0.15					
Strict			ΔVIS ΔFTs NLSD	4.0 % 5.0 K 0.1		DCD ΔFTs LSD	-1.9 K 5.0 K 0.8 K	-3.0 K 5.0 K 0.1 K

3. RESULTS

3.1 Results of HFDA using Himawari-8

Figure 4 shows the fog detection results using HFDA for the daytime and nighttime with COMS image and visibility data. The visual comparison of fog detection results with the ground observed visibility data showed that most of fog over land are well detected. The fog detection level of HFDA over land is much better than that of COMS as shown in Fig. 4d, Fig. 4e and Fig. 4f. However, especially on sea, the HFDA over-detects the fog compared to COMS as shown in Figs. 4a, 4b, and 4c in nighttime.

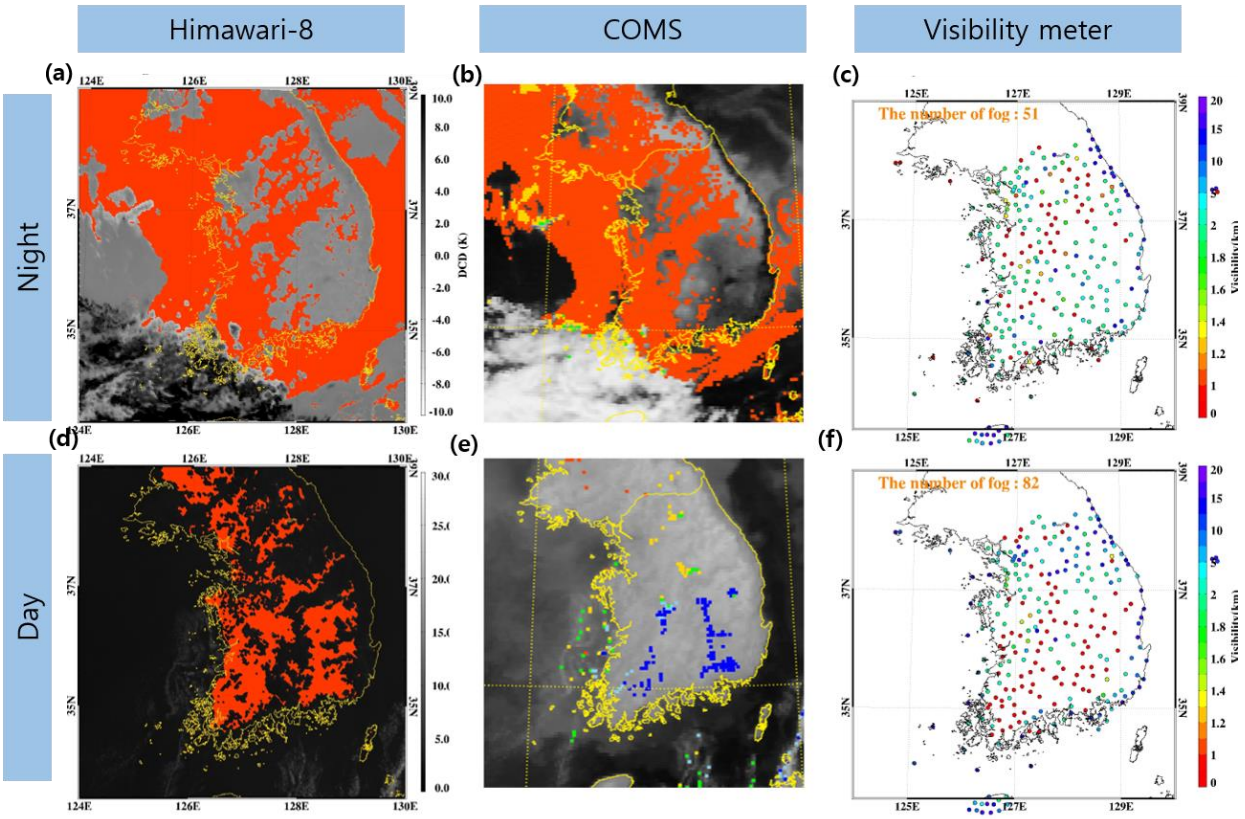

Figure 4. Sample images of fog detection results of training cases at 04:30 KST Jul. 13, 2017 and at 07:30 KST Oct. 25, 2017. (a) and (d) are results of HFDA overlapped with visible channel(03 band) and DCD image of Himawari-8/AHI, (b) and (e) are results of COMS, and (c) and (f) are ground observed visibility.

The performance of HFDA is clearly depend on the time of day, in day similar at land and coastal area, but in night and dawn better at land than coastal area. Also, the performance is greater in the training cases than that of validation cases. As shown in Figs. 5 and 6, the performance of the HFDA is significantly better at land than coast during dawn time irrespective of training and validation cases. In general, the performance is reasonable in autumn but not good in summer. It may be caused by the size and intensity of fog and atmospheric conditions. The size and intensity of fog in summer are small and weak, respectively. In addition, partly cloudy or semi-transparent cirrus are more frequent in summer.

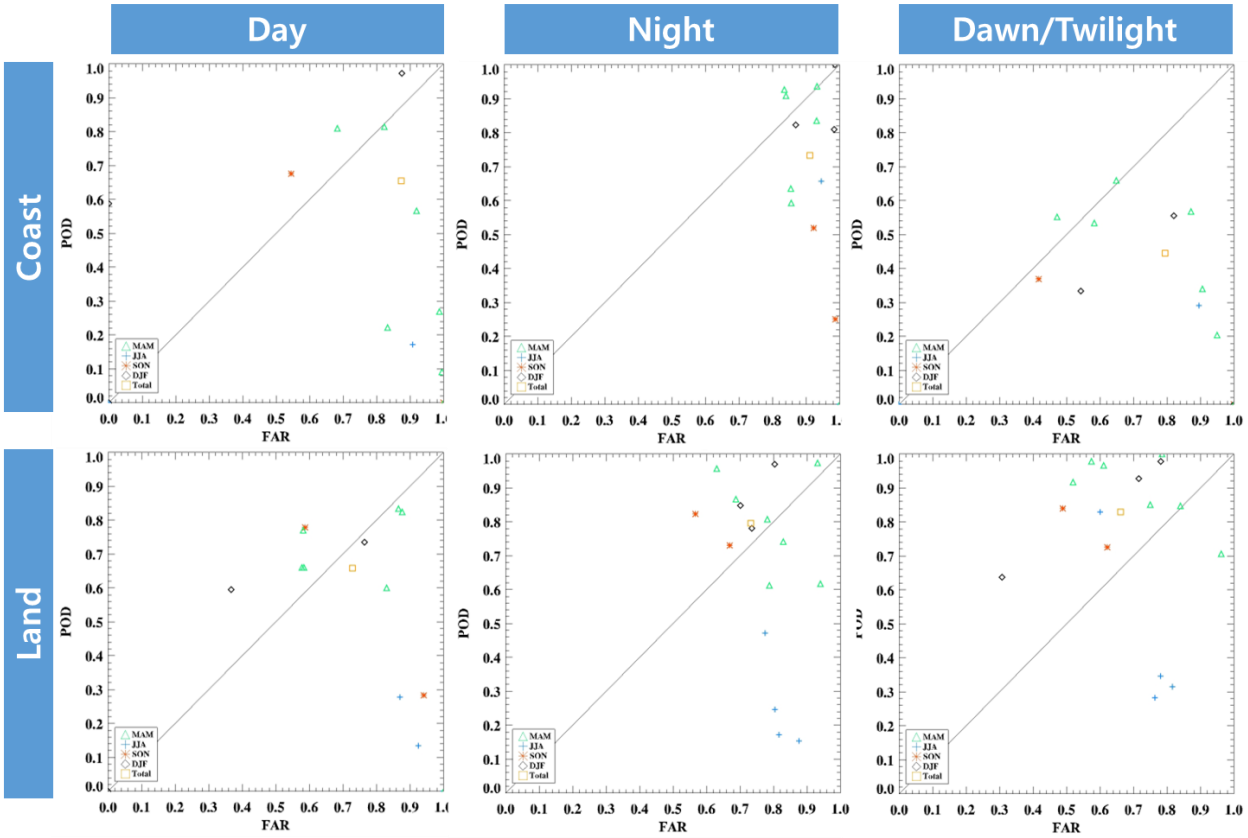

Figure 5. Scatter plot of validation results for 16 training cases according to time and geographic location. Each colored point mean the averaged POD and FAR for the selected training cases.

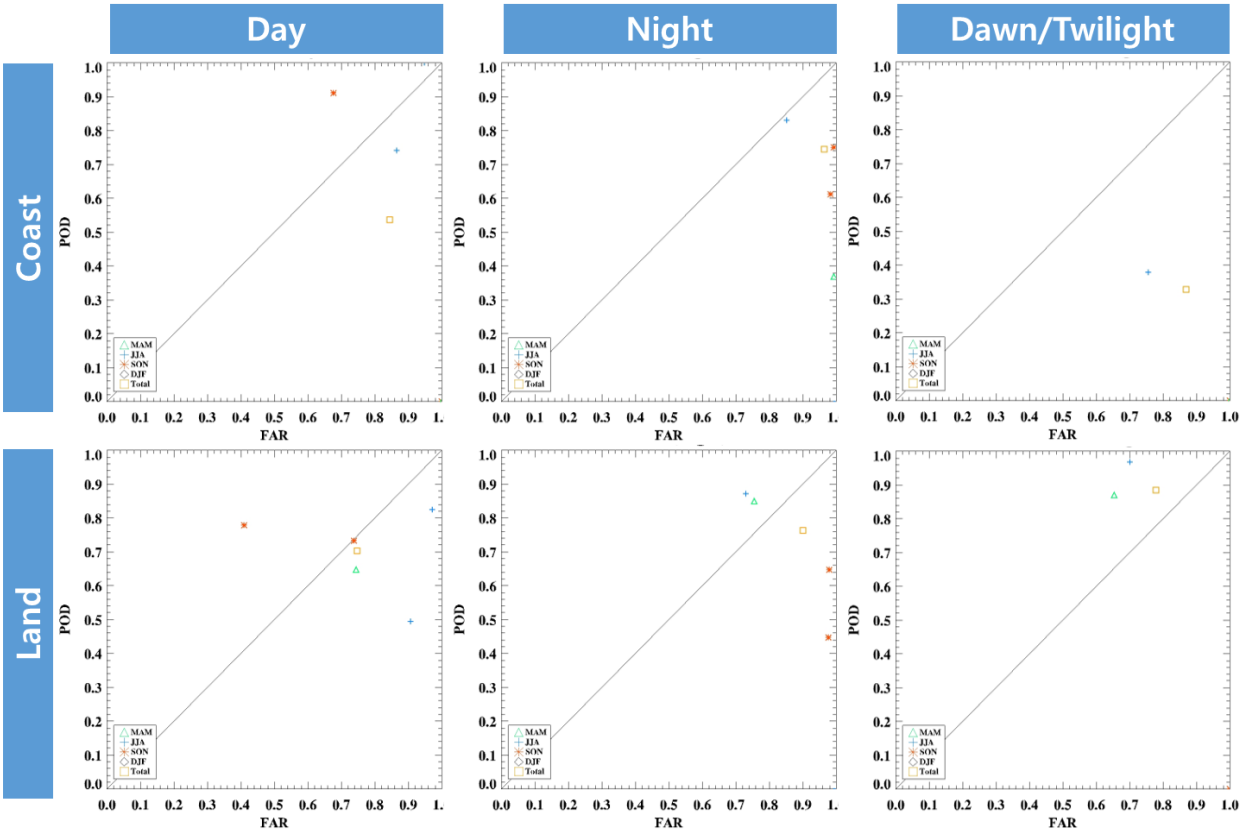

Figure 6. Same as Fig.5 except for 6 validation cases.

3.2 Results of HFDA using GK2A

The visual inspection of fog detection results with the ground observed visibility data confirmed that most of fog over land and sea are well detected.

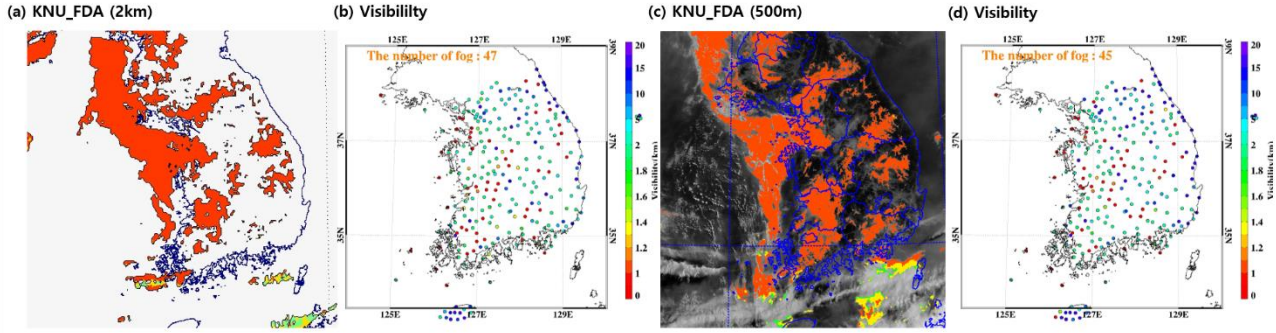

Fig. 7. Sample images of fog detection results of GK2A at 05:30 KST and 07:00 KST Jul. 04, 2019. (a) and (c) are results of HFDA for 2 km and 500 m using GK2A, respectively. (b) and (d) show the ground observed visibility for the same time

4. SUMMARY

In this study, we developed fog detection algorithm for GK2A/AMI and Himawari-8/AHI which are superior in number of channels, spatio-temporal and spectral resolutions to the previous geostationary satellites. Fog detection was performed according to SZA of pixel because of the different availability of satellite data. In addition, we divided the land, sea, and coast in order to overcome the geographical complexity of the Korea Peninsula. To determine the threshold values of test elements, 16 training cases and 6 validation cases were used. The threshold values of each test elements were selected by the visual inspection of frequency distribution and optimized through sensitivity tests for the training cases. Visual inspection showed that the HFDA similarly detected the fog for the Himawari-8/AHI and GK2A/AMI data. The validation with ground visibility data showed promising results, the averaged POD and FAR for the training and validation cases are 0.74~0.77 and 0.77~0.89, respectively. The HFDA shows a high level of detection, especially at land during spring and autumn when fog is relatively strong. It is interesting that the HFDA shows a better performance at land than coast during dawn time irrespective of training and validation cases. The detection levels are clearly dependent on the geographic location and time. Therefore, more works are needed for the operational detection of fog using GK-2A/AMI data.

5. REFERENCE

Ahn, M.H., E.H. Sohn, and B.J. Hwang, 2003. A new algorithm for sea fog/stratus detection using GMS-5 IR data. Advances in Atmospheric Sciences, 20(6), pp. 899-913.

Bessho, K., K. Date, M. Hayashi, A. Ikeda, T. Imai, H. Inoue, Y. Kumagai, T. Miyakawa, H. Murata, T. Ohno, A. Okuyama, R. Oyama, Y. Sasaki, Y. Shimazu, K. Shimoji, Y. Sumida, M. Suzuki, H. Taniguchi, H. Tsuchiyama, D. Uesawa, H. Yokota, and R. Yoshida, 2016. An introduction to Himawari-8/9—Japan's new-generation geostationary meteorological satellites, Journal of the Meteorological Society of Japan, 94(2), pp. 151-183.

Choi, Y.S. and C.H. Ho, 2015. Earth and environmental remote sensing community in South Korea: A review, Remote Sensing Applications: Society and Environment, 2, pp. 66-76.

Ellrod, G.P., 1995. Advances in the detection and analysis of fog at night using GOES multispectral infrared imagery. Weather and Forecasting, 10(3), pp. 606-619.

Eyre, J.R., J.L. Brownscombe, R.J. Allam, 1984. Detection of fog at night using advanced very high resolution radiometer (AVHRR) imagery. Meteorological Magazine. 113, pp. 266–271.

Gultepe, I., M.D. Muller, and Z. Boybeyi, 2006. A new visibility parameterization for warm-fog applications in numerical weather prediction models, Journal of Applied Meteorology Climatology, 45(11), pp. 1469-1480.

Han, J. H., M. S. Suh, S. H. Kim, 2019. Development of Day Fog Detection Algorithm Based on the Optical and Textural Characteristics Using Himawari-8 Data. Korean Journal of Remote Sensing, 35(1), pp. 117-136.

Jeon, J.Y., S.H. Kim, and C.S. Yang, 2016. Fundamental research on spring season daytime sea fog detection using

MODIS in the yellow sea, Korean Journal of Remote Sensing, 32(4), pp. 339-351.
Kim, S.H., M.S. Suh, and J.H. Han, 2018. Development of Fog Detection Algorithm during Nighttime Using Himawari-8/AHI Satellite and Ground Observation Data, Asia-Pacific Journal of Atmospheric Sciences, pp. 1-14.
Lee, H.D. and J.B. Ahn, 2013. Study on classification of fog type based on its generation mechanism and fog predictability using empirical method, Atmosphere, 23(1), pp. 103-112.
Lee, H.K and M.S. Suh, 2018. A Comparative Study on the Visibility Characteristics of Naked-Eye Observation and Visibility Meters of Fog over South Korea. Atmosphere, 28(1), pp. 69-83.
Lee, J.R., C.Y. Chung, and M.L. Ou, 2011. Fog detection using geostationary satellite data: Temporally continuous algorithm. Asia-Pacific Journal of Atmospheric Sciences, 47(2), pp.113-122.
Lee, S.J. 2016. Development of fog detection algorithm based on the optical and textural properties of fog using COMS data, Kongju National University, Kongju, Korea
NMSC, 2019. http://210.125.45.79/homepage/html/base/cmm/selectPage.do?page=static.satllite.introGk2a, Accessed on Sep. 02, 2019.
Park, H.M., and J.H. Kim, 2012. Detection of Sea Fog by Combining MTSAT Infrared and AMSR Microwave Measurements around the Korean peninsula. Atmosphere, 22(2), pp. 163-174
Park, W.S. 2012. Improvement of Fog Detection Algorithm from COMS Data, Kongju National University, Kongju, Korea
Schreiner, A. J., S. A. Ackerman, B. A. Baum, and A. K. Heidinger, 2007. A multispectral technique for detecting low-level cloudiness near sunrise. Journal of Atmospheric and Oceanic Technology, 24(10), pp. 1800-1810.
Shin, D.G., H.M., Park, and J.H., Kim, 2013. Analysis of the Fog Detection Algorithm of DCD Method with SST and CALIPSO Data. Atmosphere, 23(4), pp. 471-483.
Suh, M.S., S.J. Lee, S.H. Kim, J.H. Han, and E.K. Seo, 2017. Development of Land fog Detection Algorithm based on the Optical and Textural Properties of Fog using COMS Data, Korean Journal of Remote Sensing, 33(4), pp. 359-375.